BMC Anesthesiology

RESEARCH Open Access

Effects of propofol on the electrophysiological properties of glutamatergic neurons in the ventrolateral medulla of mice

Ya Chen[1,2,3], Tian Yu[2,3*] and Junli Jiang[1,2,3*]

Abstract

Background Propofol, a commonly used intravenous anesthetic, is associated with various respiratory adverse events, most notably different degrees of respiratory depression, which pose significant concerns for patient safety. Respiration is a fundamental behavior, with the initiation of breathing in mammals dependent on neuronal activity in the lower brainstem. Previous studies have suggested that propofol-induced respiratory depression might be associated with glutamatergic neurons in the pre-Bötzinger complex (preBötC), though the precise mechanisms are not well understood. In this study, we classify glutamatergic neurons in the brainstem preBötC using whole-cell patch-clamp techniques and investigate the effects of propofol on the electrophysiological properties of these neurons. Our findings aim to shed light on the mechanisms of propofol-induced respiratory depression and provide new experimental insights.

Methods We first employed electrophysiological techniques to classify glutamatergic neurons within the preBötC as Type-1 or Type-2. Following this classification, we applied varying concentrations of propofol through bath application to examine its effects on the electrophysiological properties of each type of glutamatergic neuron.

Results We found that Type-1 neurons exhibited a longer latency in excitation, while Type-2 neurons did not show this delayed excitation. On this basis, we further observed that bath application of propofol at concentrations of 5 μM and 10 μM shortened the latency period of Type-1 glutamatergic neurons but did not affect the latency period of Type-2 glutamatergic neurons.

Conclusion Our study focuses on the glutamatergic neurons in the preBötC of adult mice. It introduces a novel method for classifying these neurons and reveals how propofol affects the activity of the two different types of glutamatergic neurons within the preBötC. These findings contribute to understanding the cellular basis of propofol-induced respiratory depression.

Keywords pre-Bötzinger complex, Propofol, Glutamatergic neurons

*Correspondence:
Tian Yu
zyyutian@126.com
Junli Jiang
314887347@qq.com

[1]Department of Anesthesiology, Affiliated Hospital of Zunyi Medical University, Zunyi, China
[2]Guizhou Key Laboratory of Anesthesia and Organ Protection, Zunyi Medical University, Zunyi, China
[3]Guizhou Key Laboratory of Brain Science, Zunyi Medical University, Zunyi, China

Introduction

Rhythmic respiratory activity is crucial for maintaining normal physiological functions and is generated by central respiratory pattern generators, primarily located in the preBötC [1]. Neuronal populations within the preBötC constitute a crucial component of respiratory rhythmogenesis, comprising primarily glutamatergic excitatory neurons, alongside subpopulations of glycinergic and gamma-aminobutyric acid inhibitory neurons. Excitatory and inhibitory neurons are roughly equal in number [2].

Previous studies have found that microinjection of glutamate analogs into the preBötC induces respiratory responses such as apneusis and/or rapid breathing [3–6]. Targeted ablation of glutamatergic neurons expressing neurokinin 1 receptors (NK1R) in the preBötC of rats results in respiratory pauses during sleep and dysrhythmic breathing during wakefulness [7]. Prior research combining optogenetics with electrophysiology has demonstrated that optogenetic inhibition of glutamatergic neurons in the preBötC significantly disrupts inspiratory rhythm generation [8]. Taken together, glutamatergic neurons in the preBötC are central to rhythmogenesis.

During procedural sedation with propofol in clinical settings, respiratory depression affects a significant proportion of patients, ranging from 64–70% [9]. Research suggests that propofol suppresses the frequency of inspiratory bursts in the C4 phrenic nerve root, a phenomenon reversible by $GABA_A$ receptor antagonists. Moreover, propofol hyperpolarizes membrane potentials of both inspiratory and expiratory neurons, thereby reducing neuronal discharge [10]. Our previous research in the preBötC demonstrated that propofol, at a concentration of 5 μM, significantly increases the frequency of spontaneous excitatory postsynaptic current (sEPSC) and the amplitude of miniature excitatory postsynaptic currents (mEPSC). In contrast, a higher concentration of 10 μM produces an inhibitory effect. Furthermore, propofol increases the number of c-Fos positive neurons in the preBötC in a dose-dependent manner, with higher doses enhancing the activation of GABAergic neurons [11, 12]. Collectively, these studies indicate that propofol-induced respiratory depression may involve neurons in the preBötC that regulate respiratory function.

Previous studies have investigated the developing brain homeobox 1 (Dbx1) neurons in the respiratory neural network, classifying neurons into Type-1 and Type-2 based on latency periods [13]. Type-1 neurons influence respiratory frequency, while Type-2 neurons affect tidal volume, highlighting distinct roles and contributions within respiratory regulation by different Dbx1 neuron types. Furthermore, Dbx1 neurons in the preBötC are glutamatergic [14]. Therefore, we hypothesized that glutamatergic neurons in the preBötC may exhibit subtypes similar to those identified in Dbx1 neurons elsewhere, suggesting that propofol could potentially modulate respiratory rhythm generation by influencing different types of glutamatergic neurons. In this study, we employed whole-cell patch clamp techniques to categorize glutamatergic neurons in the preBötC based on their electrophysiological characteristics. Additionally, we examined the electrophysiological effects of varying concentrations of propofol on these two types of glutamatergic neurons in the preBötC.

Methods

Mice

Adult Vglut2-ires-Cre mice (Jackson Stock No. 016963) were crossed with Rosa26R-tdTomato mice (Jackson Stock No. 007908) to generate Vglut2-cre-Ai14 mice. A total of 20 Vglut2-cre-Ai14 mice, aged 3 to 6 weeks, were used for the experiments. All mice were housed in the Animal Experimental Center of Zunyi Medical University under standard conditions: temperature was maintained at 24±1 °C, humidity at 60±2%, and a 12-hour light/12-hour dark cycle (lights on from 8:00 to 20:00) was followed. Mice had ad libitum access to food and water and were allowed free movement. Experimental procedures were conducted in accordance with the guidelines of the Institutional Animal Ethics Committee. Ethics approval number: ZMU21-2203-011.

Brainstem slices and whole-cell patch-clamp recording

Mice aged 3 to 6 weeks were anesthetized with 2% isoflurane, a rapidly acting and highly controllable inhalation anesthetic that is quickly metabolized. Isoflurane has minimal suppressive effects on the circulatory and respiratory systems, which helps to maintain stable physiological conditions and reduces potential interference with neuronal activity during brainstem slice preparation, thereby ensuring the reliability of experimental results. Following anesthesia, the mice underwent cardiac perfusion with artificial cerebrospinal fluid (ACSF) until the liver turned pale gray, after which they were immediately decapitated. The brain tissue was then quickly dissected in ice-cold, continuously oxygenated (95% O2 and 5% CO2) ACSF. The composition of ACSF was as follows (in mM): 46 NMDG, 2.5 KCl, 1.25 NaH_2PO_4, 5 $MgSO_4$, 2 $CaCl_2{\cdot}2H_2O$ (1 M), 15 $NaHCO_3$, 11.4 Glucose, 1 Thiourea, 2.5 Na-ascorbate, 1.5 Na-pyruvate, 10 HEPES. After preparation, the pH of the solution was adjusted to 7.3–7.4 using concentrated hydrochloric acid. The brain tissue was then secured, with the rostral side up, on the base of a vibrating microtome (Leica, Germany) and promptly transferred to the slicing chamber. Here, the preBötC was positioned at the cutting surface. Anatomical landmarks from the literature [15] were used to locate the preBötC, which is situated ventral to the nucleus ambiguus and

lateral to the inferior olive (Fig. 1A). Coronal brain slices, 265 μm thick, were then cut and placed in a pre-warmed brainstem slice incubation chamber containing ACSF with the previously mentioned composition (in mM). The slices were incubated at 35 °C for approximately 9 min. Following this, they were allowed to recover for 60 min at room temperature in ACSF containing 91.93 NaCl, 2.5 KCl, 1.25 NaH_2PO_4, 10 HEPES, 11.4 Glucose, 1 thiourea, 2.5 Na-ascorbate, 2 $MgSO_4$, 2 $CaCl_2{\cdot}2H_2O$ (1 M), and 15 $NaHCO_3$, with continuous oxygenation maintained throughout the procedure.

The ACSF containing (in mM) 119 NaCl, 2.5 KCl, 1.25 NaH_2PO_4, 12.5 Glucose, 5 $MgSO_4$, 2 $CaCl_2{\cdot}2H_2O$ (1 M), and 11.99 $NaHCO_3$ was continuously perfused at a rate of 3–5 ml/min into the brainstem slices, supplemented with a mixture of oxygen. Following the previously described method, the preBötC was located under low magnification (Fig. 1B), after which the magnification was increased to identify cells expressing the fluorescent protein under excitation light (Fig. 1C-D). Whole-cell patch-clamp recordings were then performed using the MultiClamp 700B patch-clamp system. Patch

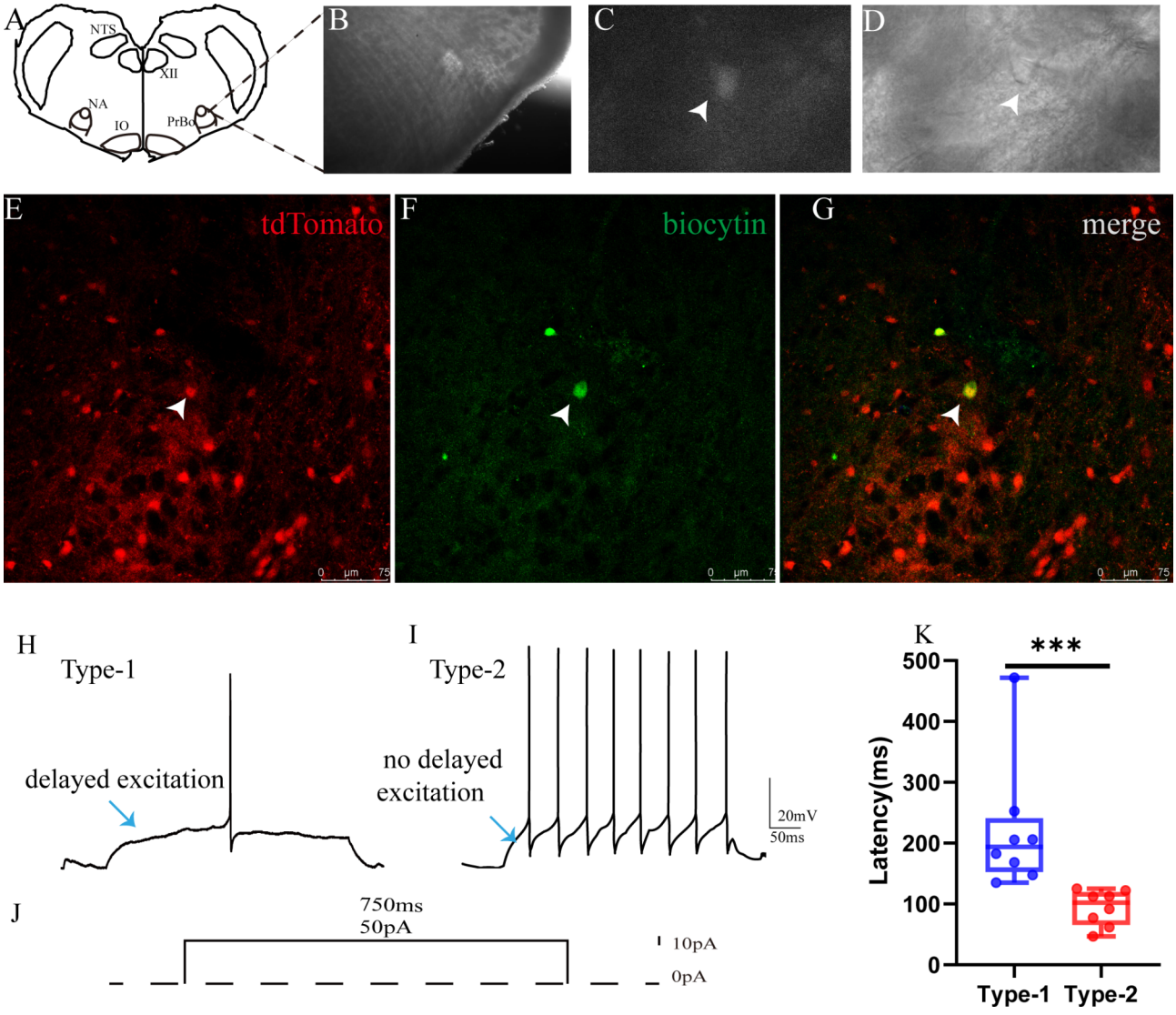

Fig. 1 Slice preparation and electrophysiological characteristics of glutamatergic neurons in the preBötC of Vglut2-cre-Ai14 mice. **A**: Configuration for recording activity of preBötC glutamatergic neurons. **B**: Schematic of a transverse slice containing the preBötC under low magnification. **C**: Fluorescent protein-expressing cells under excitation light microscopy. **D**: Clamped fluorescent cell, with the shadow of the patch pipette visible in the lower right corner. **E**. Visualization of glutamatergic neurons labeled with tdTomato. **F**. Biotin-stained glutamatergic neurons. **G**. Overlay showing tdTomato and biotin staining in glutamatergic neurons. **H**. Schematic representation of Type-1 neurons exhibiting latency excitation. **I**. Schematic representation of Type-2 neurons without latency excitation. **J**. Diagram illustrating the protocol for current injection (0pA, 10pA, 20pA, 30pA, 40pA, 50pA) into glutamatergic neurons. **K**. Statistical analysis of latency periods for Type-1 and Type-2 neurons during ACSF bath application. ***$P \leq 0.001$. PrBo: preBötC; NA: nucleus ambiguous; IO: inferior olive; XII: hypoglossal nucleus; NTS: nucleus tractus solitarius

pipettes (3–5 MΩ) were filled with an internal solution containing (in mM): 120 K-gluconate, 5 KCl, 5 NaCl, 2 $MgCl_2 \cdot 6H_2O$, 10 HEPES, 11 EGTA, 2 ATP-Mg, 1 GTP-Na, 1 $CaCl_2 \cdot 2H_2O$, and 0.2% biocytin, adjusted to a pH of 7.3 with an osmolarity of 290–300 mOsm/L. Recordings were made for 1 s from each cell under current-clamp mode, with the membrane potential clamped at -70 mV. Cells were stimulated with currents ranging from 0 pA to 50 pA (600–750 ms duration, 10 pA steps). After allowing the cells to stabilize for 5 min, an initial action potential was recorded as a baseline. Following this, propofol was diluted in ACSF to a final concentration of 5 μM or 10 μM and applied for 3 min, during which a second action potential was recorded. Finally, cells were washed with ACSF for 10 min. In this study, the same group of previously classified glutamatergic neurons (Type-1 and Type-2) was used for subsequent experiments with identical concentrations of propofol to ensure data consistency. A total of 33 Type-1 cells and 19 Type-2 cells were included.

Biotinylation staining

Following completion of electrophysiological recordings, brainstem slices were collected and fixed in a 4% paraformaldehyde solution overnight at 4 °C. The fixed brainstem slices were then rinsed three times for 5 min each in 0.1 M PBS with agitation. Subsequently, the slices were incubated in 0.3% H_2O_2 (diluted in methanol) for 30 min, followed by three washes with 0.1% PBST for 5 min each. Next, the brainstem slices were incubated in 3% non-fat milk for 1 h, followed by blocking with 10% goat serum for 1 h. Following blocking, 1% cholera toxin subunit-FITC (Sigma S3762) diluted at 1:500 was applied onto the brainstem slices and incubated in the dark for over 2 h. Recorded neurons were subsequently visualized using a fluorescence microscope (BX51W1-IR7, Olympus, Japan).

Data analyses

Electrophysiological data were collected and initially processed using Clampfit 10.7 software. Subsequent statistical analyses were conducted with SPSS 29.0 and GraphPad Prism 8.0.2. Specifically, for the rheobase comparisons of Type-2 neurons before and after the application of 5 μM propofol, the data followed a normal distribution and were analyzed using a paired t-test. The results were presented as mean ± standard deviation. In contrast, for data that did not meet the assumption of normality, the latency of Type-1 and Type-2 neurons was evaluated using the non-parametric Mann-Whitney U test. The remaining non-normally distributed data were analyzed with the Wilcoxon Signed-Rank Test, and medians (Me) were reported. In all analyses, a P value of <0.05 was considered statistically significant.

Results

Electrophysiological classification of glutamatergic neurons: Type-1 and Type-2

In the preBötC, we selectively recorded glutamatergic neurons to measure intrinsic membrane properties, specifically latency to excitation. Figure 1 shows tdTomato and biocytin-labeled glutamatergic neurons (Fig. 1E-G), confirming recordings from the targeted neurons. Following methods referenced from Christopher A. Del Negro et al. [16], each neuron underwent current clamp recordings, revealing two distinct types of glutamatergic neurons in the preBötC based on latency duration, classified as Type-1 and Type-2. The electrophysiological results revealed a significant difference in delayed excitation between Type-1 neurons (Me = 194.1 ms) and Type-2 neurons (Me = 102.1 ms). This difference was observed when depolarizing current stimuli of 0 pA, 10 pA, 20 pA, 30 pA, 40 pA, and 50 pA were applied, starting from a membrane potential of -70 mV ($P=0.001$, $n=8$; Fig. 1H-J). $n=8$ indicates that each type of glutamatergic neuron (Type-1 and Type-2) includes 8 cells.

Bath application of low concentrations of propofol shortened the latency period of Type-1 neurons

To investigate the effects of propofol on two types of glutamatergic neurons, we first examined its impact at low concentrations. Whole-cell patch-clamp recordings demonstrated a significant reduction in the latency of glutamatergic Type-1 neurons following bath application of 5 μM propofol (Me = 167.25 ms) compared to baseline (Me = 206.5 ms, $P=0.044$, $n=16$; Fig. 2A). However, the rheobase (Me = 20 pA) showed no significant change from the baseline value (Me = 20 pA, $P=0.334$, $n=16$; Fig. 2B). In contrast, bath application of 5 μM propofol, the latency of Type-2 neurons (Me = 102.1 ms) remained similar to the baseline value (Me = 96 ms, $P=1.00$, $n=8$; Fig. 2C). Likewise, the rheobase (25 ± 15.12 pA) showed no significant difference when compared to baseline (27.5 ± 14.88 pA, $P=0.351$, $n=8$; Fig. 2D). These results indicate that bath application of 5 μM propofol enhances excitability in Type-1 neurons of the preBötC while leaving Type-2 neuron excitability unaffected.

Bath application of high concentrations of propofol shortened the latency period of Type-1 neurons

Next, we administered 10 μM propofol to two types of glutamatergic neurons in the preBötC. Bath application of 10 μM propofol resulted in a significant shortening of the latency in Type-1 neurons (Me = 167.6 ms) compared to normal ACSF conditions (Me = 360.7 ms, $P=0.009$, $n=17$; Fig. 3A). In contrast, the rheobase (Me = 20 pA) remained consistent with the baseline value (Me = 20 pA, $P=0.564$, $n=17$; Fig. 3B). On the other hand, bath application of 10 μM propofol did not produce a significant

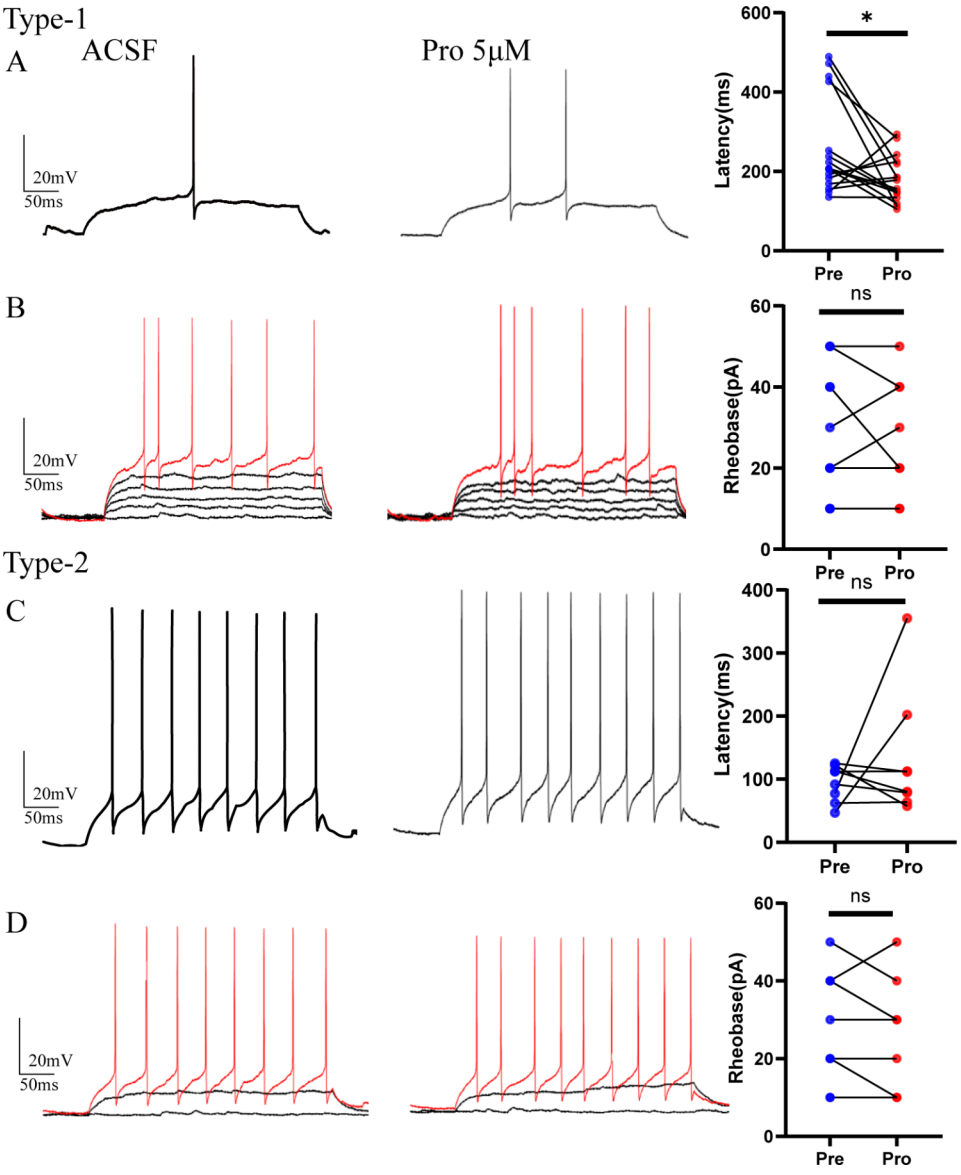

Fig. 2 Effects of bath application of low concentrations of propofol on two types of neurons. (**A**) Representative diagrams illustrating the impact of 5 μM propofol on Type-1 latency period (left: schematic during ACSF bath application, middle: schematic during 5 μM propofol bath application, right: statistical graph comparing latency periods during ACSF and propofol (5 μM) bath application). (**B**) Representative diagrams depicting the effect of 5 μM propofol on Type-1 rheobase current (left: schematic during ACSF bath application, middle: schematic during 5 μM propofol bath application, right: statistical graph comparing rheobase current during ACSF and propofol (5 μM) bath application). (**C**) Representative diagrams showing the effect of 5 μM propofol on Type-2 latency period (left: schematic during ACSF bath application, middle: schematic during 5 μM propofol bath application, right: statistical graph comparing latency periods during ACSF and propofol (5 μM) bath application). (**D**) Representative diagrams illustrating the impact of 5 μM propofol on Type-2 rheobase current (left: schematic during ACSF bath application, middle: schematic during 5 μM propofol bath application, right: statistical graph comparing rheobase current during ACSF and propofol (5 μM) bath application). Each line represents changes in an individual neuron before and after treatment, with each point indicating data from a single neuron. *$P < 0.05$

change in the latency of Type-2 neurons (Me=94.3 ms) when compared to the baseline (Me=120.3 ms, $P=0.062$, $n=11$; Fig. 3C). Similarly, the rheobase (Me=10 pA) showed no noticeable difference from the baseline value (Me=10 pA, $P=0.059$, $n=11$; Fig. 3D). These findings indicate that bath application of 10 μM propofol increases excitability of Type-1 neurons in the preBötC without affecting Type-2 neurons. Notably, different brainstem slices were used for experiments with varying concentrations of propofol, resulting in differences in baseline latency and sample size compared to the 5 μM condition.

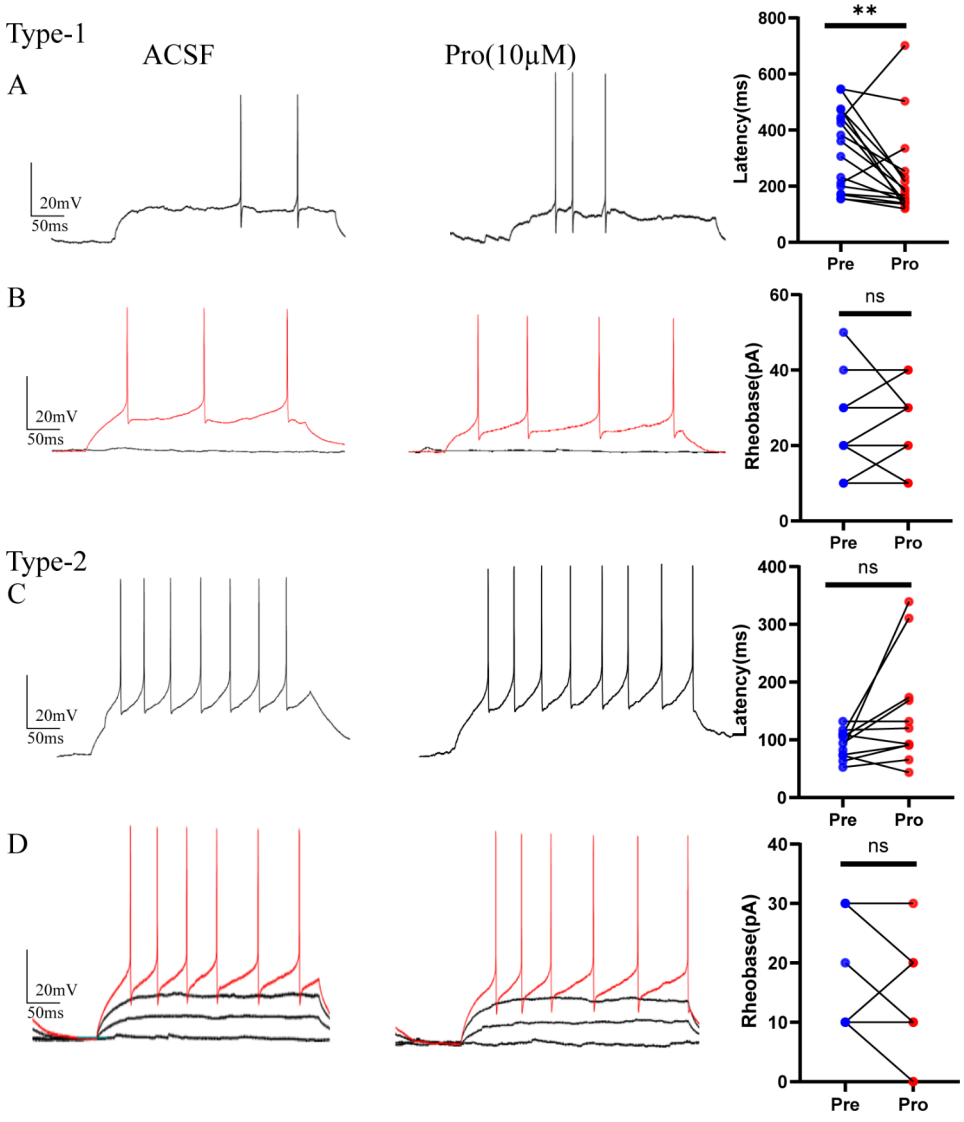

Fig. 3 Effects of bath application of high concentrations of propofol on two types of neurons. (**A**) Illustration depicting the impact of 10 μM propofol on Type-1 latency period (Left: ACSF bath application, Middle: 10 μM propofol bath application, Right: Statistical plot comparing latency periods under ACSF and 10 μM propofol conditions). (**B**) Diagram illustrating the effect of 10 μM propofol on Type-1 rheobase current (Left: ACSF bath application, Middle: 10 μM propofol bath application, Right: Statistical plot comparing rheobase current under ACSF and 10 μM propofol conditions). (**C**) Representation showing the effect of 10 μM propofol on Type-2 latency period (Left: ACSF bath application, Middle: 10 μM propofol bath application, Right: Statistical plot comparing latency period under ACSF and 10 μM propofol conditions). (**D**) Diagram illustrating the impact of 10 μM propofol on Type-2 rheobase current (Left: ACSF bath application, Middle: 10 μM propofol bath application, Right: Statistical plot comparing rheobase current under ACSF and 10 μM propofol conditions). Each line represents changes in an individual neuron before and after treatment, with each point indicating data from a single neuron. $^{**}P < 0.01$

Discussion

Glutamatergic neurons, predominantly excitatory, play crucial roles in mammalian physiology, influencing cardiovascular regulation, respiratory signaling, motor functions, and social behavior. In previous studies, glutamatergic neurons have been differentiated based on the expression of various molecular markers, including somatostatin (SST) [2], neurokinin-1 receptor (NK1R) [17], and types I, II, and III vesicular glutamate transporters (Vglut1, Vglut2, Vglut3). However, Vglut3 frequently colocalizes with other molecular markers in specific nuclei [18], limiting its reliability as a definitive marker for glutamatergic neurons. In the preBötC, excitatory glutamatergic neurons primarily express Vglut2 [19]. Due to the absence of clear anatomical boundaries, neurons labeled with these molecular markers cannot be strictly confined to the preBötC. From a genetic perspective, excitatory glutamatergic neurons in the preBötC have been further identified as Dbx1 neurons [20], which

provides valuable insights into neuronal microcircuit function.

In this study, we classified glutamatergic neurons as Type-1 and Type-2 based on their electrophysiological properties, with Type-1 neurons displaying a longer latency period than Type-2 neurons, indicating differences in neuronal excitability. The application of propofol (5 μM and 10 μM) further shortened the latency period in Type-1 neurons but had no effect on the latency period of Type-2 neurons or the rheobase current in either type. Our experiment expands upon the work of Christopher A. Del Negro et al. [16], who studied Dbx1 neurons in the preBötC of neonatal mice, by extending the focus to glutamatergic neurons in the preBötC of adult mice. By identifying and demonstrating differences in the electrophysiological properties of these neuron types in adult animals, our study provides a foundation for exploring the targets and mechanisms of propofol-mediated central respiratory depression under general anesthesia.

Propofol-induced excitation of glutamatergic neurons in the preBötC

The in vitro brainstem preparation is widely used to analyze the effects of drugs on central respiratory control. In this model, propofol concentrations of 5 μM and 10 μM are commonly applied to investigate the mechanisms underlying general anesthesia. Previous studies have demonstrated that 1 μM propofol does not affect the electrophysiological properties of medullary brainstem neurons [21], whereas higher concentrations, such as 20 μM, lead to an 80% incidence of respiratory depression [10]. Based on this, we selected concentrations of 5μM and 10 μM, which allows for effective observation of neuronal activity while avoiding complete respiratory inhibition. Clinically, the concentration of propofol in cerebrospinal fluid stabilizes at levels as low as 52 ng/mL (0.00029 μM) [22], which is significantly lower than the concentrations used in our bath solution. This difference can be attributed to several factors, including the slow diffusion rate of propofol in vitro brain tissue slices (0.02×10^{-6} cm^2s^{-1}), species-specific variations, and the lack of blood perfusion in isolated brain tissue [23]. These factors result in the actual concentration within brain tissue being much lower than that of the bath solution. Consequently, we chose the propofol concentrations for this study based on previous research findings [10, 24].

Previous studies focused on the lateral hypothalamus [25] and basal forebrain [26] have demonstrated that propofol induces unconsciousness by enhancing GABAergic inhibition onto glutamatergic neurons, thereby reducing their excitability. However, other research indicates that propofol can increase excitability of glutamatergic neurons. For example, propofol enhances the excitability of glutamatergic neurons in the lateral hypothalamus, leading to sedation, and blocking glutamatergic output significantly diminishes propofol's sedative effects [27]. Moreover, propofol has been found to elevate the activity of glutamatergic neurons in the piriform cortex, resulting in behavioral deficits in mice [28]. These insights underscore the nucleus-specific effects of propofol-induced alterations in glutamatergic neuron excitability.

Neurons in the preBötC contain ligand-gated ion channels that mediate rapid GABAergic synaptic transmission. $GABA_A$ receptors are located not only on the postsynaptic membrane but also on the presynaptic membrane. Studies have shown that, in the NTS, propofol (at concentrations ≥ 3 μM) increases the frequency of sEPSC in a concentration-dependent manner, triggering glutamate release from synaptic terminals via presynaptic depolarization mediated by $GABA_A$ receptors [21]. This aligns with our previous findings that propofol exerts presynaptic effects, dose-dependently suppressing the frequency of sEPSC in certain nuclei [11, 12].

Neurons in the preBötC contain voltage-gated ion channels that, in addition to chemical neurotransmission, regulate neuronal excitability and serve as potential targets for general anesthesia. This study found that propofol significantly shortened the latency period of Type-1 neurons, indicating their higher sensitivity to this anesthetic. The underlying mechanisms of the differing excitability responses of Type-1 and Type-2 neurons to propofol may be associated with variations in their ion channel distributions. Previous research has shown that Type-1 Dbx1 neurons play a more crucial role in generating respiratory rhythms and exhibit greater dependence on calcium channels [16]. Building on this, we hypothesize that the differential effects of propofol on glutamatergic neurons in the preBötC are mediated through the modulation of cation currents. Our findings showed that propofol did not significantly affect the excitability of Type-2 neurons. However, there was a trend where 5 μM propofol prolonged the latency period of Type-2 neurons, though this did not reach statistical significance. In contrast, 10 μM propofol demonstrated a trend of shortening the latency of these neurons. This may indicate that the latency period of Type-2 neurons was already approaching its physiological limit, which could prevent propofol from further reducing it significantly, even when acting on similar targets. These observations suggest that the differential regulatory actions of propofol on various types of glutamatergic neurons are likely connected to their distinct physiological functions in respiratory regulation.

Changes in the activity of glutamatergic neurons in the preBötC and respiration function

In rodents, the preBötC in the ventrolateral medulla serves as the origin of respiratory rhythmogenesis,

comprising approximately 3000 neurons that share similarities with humans [29, 30]. Research has found that injection of D, L-homocysteic acid into the preBötC enhances the excitability of glutamatergic neurons, leading to robust respiratory responses such as high-frequency breathing, high-amplitude inspiratory bursts, and tonic inspiratory movements, accompanied by a decrease in mean arterial pressure. Conversely, reducing the excitability of these neurons decreases respiratory frequency and raises blood pressure [4–6, 31]. Furthermore, the activity of glutamatergic neurons in the preBötC influences cough intensity and pattern [31]. These findings underscore the crucial role of glutamatergic neuron activity in cardiovascular and pulmonary function, particularly in the regulation of respiratory function.

Research has indicated that the preBötC contains diverse neuronal subtypes, and both embryonic and adult mice show that glutamatergic neurons expressing the Dbx1 transcription factor are central to respiratory rhythm generation [32]. Building upon the established knowledge base concerning Dbx1 neurons in the preBötC, this study extensively utilizes relevant findings from previous research on this neuronal subtype. Additional investigations into Dbx1 neurons have revealed inherent differences in membrane properties between Type-1 and Type-2 Dbx1 neurons [16], which is directly pertinent to the focus of this experiment.

Further research has revealed distinct physiological characteristics between the two types of Dbx1 neurons: Type-1 neurons express transient A-type K^+ currents (I_A), while Type-2 neurons do not. In the preBötC, neurons expressing I_A currents are crucial for rhythm generation, with Type-2 neurons becoming active subsequent to Type-1 neurons to modulate respiratory motor output patterns, such as tidal volume [33]. Our study observed that propofol (5μM and 10μM) increases the excitability of Type-1 glutamatergic neurons without affecting Type-2 neurons. Therefore, we hypothesize that propofol may influence respiratory frequency by altering the activity of Type-1 glutamatergic neurons while leaving tidal volume unchanged.

Moreover, studies highlight the Gabrb3 subunit of $GABA_A$ receptors as a crucial factor in the respiratory depression responses induced by propofol [34]. Our study focused exclusively on the electrophysiological classification of glutamatergic neurons and did not include RNA sequencing of the Gabrb3 subunit in these neuronal types. This limitation may hinder a comprehensive understanding of the molecular mechanisms involved; nevertheless, our identification of their cellular characteristics lays groundwork for future research endeavors. Previous studies on respiration-related neurons have primarily focused on neonatal mice and employed high-potassium ACSF, with relatively few investigations targeting adult mice. This experiment aimed to examine the effects of propofol on respiration-related neurons in the preBötC of adult mice; therefore, the localization of the preBötC was partially based on findings from neonatal studies. Propofol primarily induces Cl^- influx by activating $GABA_A$ receptors. Research indicates that GABA undergoes a developmental shift from excitatory to inhibitory effects, with $GABA_A$ receptors exerting depolarizing excitatory effects in neonatal neurons in rodents [35]. To minimize the influence of developmental changes in neuronal properties, we conducted our experiments in adult mice, which may have contributed to our inability to record rhythmic activity in the preBötC. Future studies will involve more detailed investigations to further verify whether propofol modulates respiratory activity through the two types of glutamatergic neurons identified in this study. Given the pivotal role of the preBötC in respiration, future investigations will continue to explore how propofol affects neuronal respiratory responses in this region, providing further insights into the mechanisms underlying propofol-induced respiratory depression associated with general anesthesia.

In summary, our findings introduce a novel classification of glutamatergic neurons in the preBötC based on electrophysiological characteristics. Furthermore, we assessed the pharmacodynamic effects of propofol, revealing that it exerts distinct regulatory influences on the electrophysiological properties of the two neuron types, Type-1 and Type-2.

Abbreviations

ACSF	Artificial cerebrospinal fluid
Dbx1	Developing brain homeobox 1
IO	Inferior olive
I_A	A-type K^+ currents
mEPSC	Miniature excitatory postsynaptic currents
NA	Nucleus ambiguous
NK1R	Neurokinin 1 receptors
NTS	Nucleus tractus solitarius
PreBötC/PrBo	Pre-Bötzinger complex
sEPSC	Spontaneous excitatory postsynaptic current
SST	Somatostatin
Vglut1	Type I vesicular glutamate transporter
Vglut2	Type II vesicular glutamate transporter
Vglut3	Type III vesicular glutamate transporter
XII	Hypoglossal nucleus

Acknowledgements
Not applicable.

Author contributions
Y.C. performed experiments, conducted data analysis, and wrote the manuscript. T.Y. and J.J. designed the experiments and revised the manuscript. J.J. also provided financial support.

Funding
This work was supported by the National Natural Science Foundation of China [No:82260706 and 82201424]; The Health Commission of Guizhou Province [No: gzwkj2022-116].

Data availability
The data that support the findings of this study are available from the authors but restrictions apply to the availability of these data, which were used under license from the Guizhou Key Laboratory of Anesthesia and Organ Protection (zunyi) for the current study, and so are not publicly available. Data are, however, available from the authors upon reasonable request and with permission from the Guizhou Key Laboratory of Anesthesia and Organ Protection.

Declarations

Ethics approval and consent to participate
All animal studies were approved by the Ethics Committee of Zunyi Medical University.

Consent for publication
Not applicable.

Competing interests
The authors declare no competing interests.

Received: 22 August 2024 / Accepted: 15 November 2024
Published online: 27 November 2024

References

1. Smith JC, Ellenberger HH, Ballanyi K, et al. Pre-Bötzinger complex: a brainstem region that may generate respiratory rhythm in mammals [J]. Science. 1991;254(5032):726–9. https://doi.org/10.1126/science.1683005
2. Ashhad S, Feldman JL. Emergent elements of inspiratory rhythmogenesis: network synchronization and synchrony propagation [J]. Neuron. 2020;106(3):482–e974. https://doi.org/10.1016/j.neuron.2020.02.005
3. Stucke AG, Miller JR, Prkic I, et al. Opioid-induced respiratory depression is only partially mediated by the preBötzinger complex in young and adult rabbits. Vivo [J] Anesthesiology. 2015;122(6):1288–98. https://doi.org/10.1097/aln.0000000000000628
4. Chitravanshi VC, Sapru HN. Phrenic nerve responses to chemical stimulation of the subregions of ventral medullary respiratory neuronal group in the rat [J]. Brain Res. 1999;821(2):443–60. https://doi.org/10.1016/s0006-8993(99)01139-7
5. Mccrimmon DR, Monnier A, Hayashi F et al. Pattern formation and rhythm generation in the ventral respiratory group [J]. Clin Exp Pharmacol Physiol. 2000;27(1–2):126–31. https://doi.org/10.1046/j.1440-1681.2000.03193.x
6. Solomon IC, Edelman NH, Neubauer JA. Patterns of phrenic motor output evoked by chemical stimulation of neurons located in the pre-Bötzinger complex in vivo [J]. J Neurophysiol. 1999;81(3):1150–61. https://doi.org/10.1152/jn.1999.81.3.1150
7. Mckay LC, Feldman JL. Unilateral ablation of pre-botzinger complex disrupts breathing during sleep but not wakefulness [J]. Am J Respir Crit Care Med. 2008;178(1):89–95. https://doi.org/10.1164/rccm.200712-1901OC
8. Koizumi H, Mosher B, Tariq MF, et al. Voltage-dependent rhythmogenic property of respiratory Pre-Bötzinger complex glutamatergic, Dbx1-derived, and somatostatin-expressing neuron populations revealed by graded optogenetic inhibition [J]. eNeuro. 2016;3(3). https://doi.org/10.1523/eneuro.0081-16.2016
9. Schick A, Driver B, Moore JC, et al. Randomized clinical trial comparing procedural amnesia and respiratory depression between moderate and deep sedation with propofol in the emergency department [J]. Acad Emerg Med. 2019;26(4):364–74. https://doi.org/10.1111/acem.13548
10. Kashiwagi M, Okada Y, Kuwana SI, et al. A neuronal mechanism of propofol-induced central respiratory depression in newborn rats [J]. Anesth Analg. 2004;99(1):49–55. https://doi.org/10.1213/01.ANE.0000117226.45704.65
11. Jiang J, Jiao Y, Gao P, et al. Propofol differentially induces unconsciousness and respiratory depression through distinct interactions between GABAA receptor and GABAergic neuron in corresponding nuclei [J]. Acta Biochim Biophys Sin (Shanghai). 2021;53(8):1076–87. https://doi.org/10.1093/abbs/gmab084
12. Jiang J, Jiao Y, Gao P, et al. Corrigendum to: propofol differentially induces unconsciousness and respiratory depression through distinct interactions between GABAA receptor and GABAergic neuron in corresponding nuclei [J]. Acta Biochim Biophys Sin (Shanghai). 2023. https://doi.org/10.3724/abbs.20244135
13. Picardo MC, Weragalaarachchi KT, Akins VT, et al. Physiological and morphological properties of Dbx1-derived respiratory neurons in the pre-botzinger complex of neonatal mice [J]. J Physiol. 2013;591(10):2687–703. https://doi.org/10.1113/jphysiol.2012.250118
14. Bachmutsky I, Wei XP, Kish E, et al. Opioids depress breathing through two small brainstem sites [J]. Elife. 2020;9. https://doi.org/10.7554/eLife.52694
15. Ruangkittisakul A, Kottick A, Picardo MC, et al. Identification of the pre-Bötzinger complex inspiratory center in calibrated sandwich slices from newborn mice with fluorescent Dbx1 interneurons [J]. Physiol Rep. 2014;2(8). https://doi.org/10.14814/phy2.12111
16. Kallurkar PS, Picardo MCD, Sugimura YK, et al. Transcriptomes of electrophysiologically recorded Dbx1-derived respiratory neurons of the preBötzinger complex in neonatal mice [J]. Sci Rep. 2022;12(1):2923. https://doi.org/10.1038/s41598-022-06834-z
17. Liu YY, Wong-Riley MT, Liu JP, et al. Relationship between two types of vesicular glutamate transporters and neurokinin-1 receptor-immunoreactive neurons in the pre-Bötzinger complex of rats: light and electron microscopic studies [J]. Eur J Neurosci. 2003;17(1):41–8. https://doi.org/10.1046/j.1460-9568.2003.02418.x
18. Lin LH, Talman WT. Nitroxidergic neurons in rat nucleus tractus solitarii express vesicular glutamate transporter 3 [J]. J Chem Neuroanat. 2005;29(3):179–91. https://doi.org/10.1016/j.jchemneu.2005.01.002
19. Wallén-Mackenzie A, Gezelius H, Thoby-Brisson M, et al. Vesicular glutamate transporter 2 is required for central respiratory rhythm generation but not for locomotor central pattern generation [J]. J Neurosci. 2006;26(47):12294–307. https://doi.org/10.1523/jneurosci.3855-06.2006
20. Bouvier J, Thoby-Brisson M, Renier N, et al. Hindbrain interneurons and axon guidance signaling critical for breathing [J]. Nat Neurosci. 2010;13(9):1066–74. https://doi.org/10.1038/nn.2622
21. Jin Z, Choi MJ, Park CS, et al. Propofol facilitated excitatory postsynaptic currents frequency on nucleus tractus solitarii (NTS) neurons [J]. Brain Res. 2012;1432:1–6. https://doi.org/10.1016/j.brainres.2011.11.018
22. Dawidowicz AL, KalityŃski R, Nestorowicz A, et al. Changes of propofol concentration in cerebrospinal fluid during continuous infusion [J]. Anesth Analg. 2002;95(5):1282-4, table of contents. https://doi.org/10.1097/00000539-200211000-00033
23. Gredell JA, Turnquist PA, Maciver MB, et al. Determination of diffusion and partition coefficients of propofol in rat brain tissue: implications for studies of drug action in vitro [J]. Br J Anaesth. 2004;93(6):810–7. https://doi.org/10.1093/bja/aeh272
24. Li J, Yu T, Shi F, et al. Involvement of ventral periaqueductal gray dopaminergic neurons in propofol anesthesia [J]. Neurochem Res. 2018;43(4):838–47. https://doi.org/10.1007/s11064-018-2486-y
25. Huang Y, Xiao Y, Li L, et al. Propofol-induced anesthesia involves the direct inhibition of glutamatergic neurons in the lateral hypothalamus [J]. Front Neurosci. 2024;18:1327293. https://doi.org/10.3389/fnins.2024.1327293
26. Li Y, Chen L, Zhu D, et al. Propofol downregulates the activity of glutamatergic neurons in the basal forebrain via affecting intrinsic membrane properties and postsynaptic GABAARs [J]. NeuroReport. 2020;31(17):1242–8. https://doi.org/10.1097/wnr.0000000000001540
27. Gelegen C, Miracca G, Ran MZ, et al. Excitatory pathways from the lateral habenula enable propofol-induced sedation [J]. Curr Biol. 2018;28(4):580. https://doi.org/10.1016/j.cub.2017.12.050
28. Yu D, Xiao R, Huang J, et al. Neonatal exposure to propofol affects interneuron development in the piriform cortex and causes neurobehavioral deficits in adult mice [J]. Psychopharmacology. 2019;236(2):657–70. https://doi.org/10.1007/s00213-018-5092-4
29. Moss IR. Canadian Association of Neuroscience Review: respiratory control and behavior in humans: lessons from imaging and experiments of nature [J]. Can J Neurol Sci. 2005;32(3):287–97. https://doi.org/10.1017/s0317167100004157
30. Yang CF, Feldman JL. Efferent projections of excitatory and inhibitory pre-Botzinger complex neurons [J]. J Comp Neurol. 2018;526(8):1389–402. https://doi.org/10.1002/cne.24415
31. Shen TY, Poliacek I, Rose MJ, et al. The role of neuronal excitation and inhibition in the pre-Bötzinger complex on the cough reflex in the cat [J]. J Neurophysiol. 2022;127(1):267–78. https://doi.org/10.1152/jn.00108.2021
32. Vann NC, Pham FD, Dorst KE, et al. Dbx1 Pre-Bötzinger Complex interneurons comprise the core inspiratory oscillator for breathing in unanesthetized adult mice [J]. eNeuro. 2018;5(3). https://doi.org/10.1523/eneuro.0130-18.2018

33. Gray PA, Rekling JC, Bocchiaro CM, et al. Modulation of respiratory frequency by peptidergic input to rhythmogenic neurons in the preBötzinger complex [J]. Science. 1999;286(5444):1566–8. https://doi.org/10.1126/science.286.5444.1566
34. Zeller A, Arras M. Distinct molecular targets for the central respiratory and cardiac actions of the general anesthetics etomidate and propofol [J]. Faseb j. 2005;19(12):1677–9. https://doi.org/10.1096/fj.04-3443fje
35. Eilers J, Plant TD, Marandi N et al. GABA-mediated Ca2 + signalling in developing rat cerebellar Purkinje neurones [J]. J Physiol. 2001;536(Pt 2):429–37. https://doi.org/10.1111/j.1469-7793.2001.0429c.xd

Publisher's note